CERN - EUROPEAN ORGANIZATION FOR NUCLEAR RESEARCH

Submitted to the
International Conference
on High Energy Physics
Tbilisi, 15-21 July 1976

CERN/EP/PHYS 76-43
30 June 1976

GENERAL CHARACTERISTICS OF EVENTS WITH A PARTICLE OF LARGE TRANSVERSE MOMENTUM IN pp COLLISIONS AT $\sqrt{S}$ = 52.5 GeV

CERN-Collège de France-Heidelberg-Karlsruhe Collaboration

M. DELLA NEGRA, D. DRIJARD, H.G. FISCHER, G. FONTAINE, H. FREHSE
P. FRENKIEL, C. GHESQUIERE, R. GOKIELI, P. HANKE
P.G. INNOCENTI, W. ISENBECK, E.E. KLUGE, V. KORBEL, W. HOFMANN,
D. LINGLIN, A. MINTEN, A. NORTON, A. PUTZER, H. SCHNEIDER, R. SOSNOWSKI,
J. STIEWE, S. STEIN and D. WEGENER

ABSTRACT

Events with a particle of large transverse momentum were studied at the CERN Intersecting Storage Rings using the Split Field Magnet Facility. Events were recorded by triggering on a charged large p_T secondary in two angular regions, $\theta \simeq 20^o$ and $\theta \simeq 45^o$. Inclusive distributions for the other charged particles in large p_T events are given and compared to normal events.

In order to investigate the origin of large transverse momentum secondaries in high energy pp collisions, it is necessary to study the properties of the other secondaries produced together with the large p_T particle. The Split Field Magnet Facility (SFM) of the CERN Intersecting Storage Rings (ISR), offers the possibility to measure the momenta of the charged particles produced in an event in nearly the full solid angle; thus their rapidity, transverse momentum and azimuthal angle distribution can be studied.

The SFM detector consists of multiwire proportional chambers (MWPC) in the split field magnet having a field strengh of up to 1 Tesla and surrounding an ISR interaction region. The detector layout is shown in fig. 1.

The MWPC system was used in a selftriggering mode by requiring the signals from groups of wires to follow a given geometric pattern, i.e. a road through the chamber system containing the trajectories of charged particles of certain kinematical variables. In this way events were selected with one secondary produced in a given angular region θ^* having a large transverse momentum p_T. Details of this method have been published previously [1].

The four angular regions covered by trigger roads to select large p_T secondaries are also indicated in fig. 1 and are labelled 45° OUT (i.e. $\theta^* = 45^\circ$, outside the ISR), 20° OUT and for two regions 20° INS. In addition to the large p_T events obtained by triggering in the way described above, a sample of normal events, i.e. inelastic pp collisions, was also recorded by using a minimum bias trigger. These normal events are used for comparison purposes.

The data presented here were obtained at a c.m. energy $\sqrt{S} = 52.6$ GeV and consist of 4 different samples according to the charge and production angular region of the triggering particle. In the table we list the parameters for the respective samples.

In this paper we are going to study the rapidity distribution of secondary particles in large p_T events for different trigger conditions

and for different regions in phase space. In particular we will analyze the rapidity distribution for two regions of the angle ϕ of the secondaries where ϕ is the azimuthal angle around the axis defined by the incident beams. One region comprises secondaries with $\Delta\phi = 25^{\circ}$, where ϕ is the relative azimuthal angle with respect to the triggering particle. This region will be labelled "TOWARDS" the trigger region. Secondaries opposite in azimuthal angle to the large p_T particle constitute the second sample, labelled "AWAY" from the trigger. The limits for the latter are $\Delta\phi = 180^{\circ} \pm 40^{\circ}$.

The acceptance of the SFM detector has been calculated taking into account geometrical losses, decay and interactions of the secondaries. The distributions given below are corrected for these effects. Losses in the pattern recognition program due to nearly overlapping trajectories are still under study.

The rapidity distributions of secondaries in the azimuthal angle region towards the trigger are displayed in figs 2-5. Each of these figures shows 6 different samples according to the production angle of the large p_T particle and to the transverse momentum of the secondaries. On the left side the sample with $\theta \simeq 20^{\circ}$ is displayed, the right hand side corresponds to $\theta \simeq 45^{\circ}$. These two samples are further subdivided according to the p_T of the other secondaries accompanying the large p_T particle to yield 3 samples each: $0.3 < p_T < 0.5$ GeV/c, $0.5 < p_T < 1.0$ GeV/c and $1.0 < p_T$ GeV/c.

The following observations can be made by comparing the distributions of figs 2-5 with the equivalent distributions of normal inelastic events indicated by the full line in the respective figures:

(1) The multiplicity of charged secondaries increases in large p_T events. This increase is limited to the rapidity region close to the one of the triggering large p_T particle.

(2) This structure in the rapidity distribution becomes more pronounced as the p_T of the charged secondaries increases.

(3) The increase of multiplicity is bigger for secondaries of opposite charge as the triggering large p_T particle than for secondaries of the same charge.

(4) The increase of multiplicity is bigger for the 45^o trigger than for the 20^o trigger.

The last 2 points are illustrated in fig. 6, where the multiplicity increase for different charge combinations is given as a function of the trigger rapidity.

After having discussed the azimuthal region towards the trigger we now proceed to describe the behaviour of secondaries produced in the region away from the trigger. The relevant rapidity distributions are displayed in figs 7-10, these figures correspond to the equivalent ones for the toward region described above.

If we compare the distributions in figs 7-10 for the large p_T events with those of normal inelastic events, again indicated by the full line, the following observations can be made:

(1) There is a pronounced increase of the charged multiplicity present spreading over nearly the full rapidity interval: $-3 < y < 3$.

(2) This enhancement appears to be symmetric around $y = 0$ for all trigger conditions. Hence the emission of the "away" particles is not strongly correlated to the emission angle of the high-p_T particle.

(3) The excess of particles emitted in the away region does not depend on their absolute charge, nor on their charge relative to the triggering particle.

(4) The observed relative excess increases with the transverse momentum of the secondaries.

(5) The enhancement observed for positive particles is broader in y than for negative particles. This difference between positive and negative particles increases with their transverse momentum.

In conclusion, we have studied the variation of the rapidity distribution for different large p_T trigger conditions and different samples of secondary particles. We observe an increase in multiplicity of the charged particles both in the azimuthal angle regions towards and away from the trigger, if we compare to normal events. In the azimuthal region towards the trigger the increase is limited to a narrow rapidity interval around the rapidity of the trigger, $\Delta y \simeq \pm 0.5$, whereas opposite to the trigger it spreads over the whole kinematically allowed interval in rapidity, $y = \pm 3$. In the latter case the distribution is nearly symmetric around $y = 0$, no pronounced shift of this rapidity distribution with respect to the rapidity of the trigger is observed, in contrast to predictions of many models [2]. Moreover the rapidity distribution does not depend on the absolute charge of the secondaries nor on their relative charge with respect to the trigger, except that the rapidity distribution of negative particles is slightly narrower than the one of positive ones. The rapidity distribution for charged particles towards the trigger, on the other hand, exhibits clear charge correlations, favouring secondaries of opposite charge to the trigger. The increase of multiplicity does not depend on the absolute charges involved, however. The excess of particles towards the trigger is limited to a narrow rapidity region around the large p_T particle and moves with the trigger.

REFERENCES

[1] M. Della Negra et al., NP B104 (1976) 365.

[2] See e.g. S.D. Ellis, Raporteurs talk at the International Conference on High Energy Physics, London 1974.

FIGURE CAPTIONS

Fig. 1 Top view of the Split Field Magnet detector. The shaded areas indicate the angular regions covered by the trigger on large p_T secondaries.

Fig. 2 Rapidity distribution of negative secondaries in the "towards" azimuthal angle region and for triggering large p_T particles of positive charge. Distributions (a), (b) and (c) refer to the 20^o trigger, (d), (e) and (f) to the 45^o trigger. The distributions (a) and (d) contain secondaries in the interval $0.3 < p_T < 0.5$ GeV/c, (b) and (e) in $0.5 < p_T < 1.0$ GeV/c and (c) and (f) those with $p_T > 1.0$ GeV/c. Full line indicates the respective distribution of normal events. The vertical scale is the charged multiplicity, times 100, per interval of $\Delta\phi$ and Δy (in radian^{-1}).

Fig. 3 Same as fig. 2 but trigger particle is negative and other secondaries positive.

Fig. 4 Same as fig. 2 but trigger is negative and other secondaries are also negative.

Fig. 5 Same as fig. 2 but for positive trigger and positive secondaries.

fig. 6 The increase of charged multiplicity with respect to normal events in the azimuthal angle region "towards" trigger as a function of the rapidity of the large p_T triggering particle. Points on lower line refer to secondaries of the same charge as the trigger, on upper to those of opposite charge.

Fig. 7-10 Same as figs 2-5 but for secondaries in the azimuthal angle region "away" from the trigger.

TABLE I

Trigger name	θ^* (Trigger mean CM angle of production)	<y> Mean rapidity ± σ	Trigger azim. range/prod. plane	$\langle p_T \rangle$	<n> Mean event Mult.	Number of events on DST
45^o OUT −	$49^o.6$	0.76 ± 0.07	± 15^o	2.43	10.4	51800
45^o OUT +	$44^o.3$	0.90 ± 0.05	± 12^o	2.45	9.9	31100
20^o OUT −	$21^o.6$	1.66 ± 0.25	± 25^o	2.21	9.3	77100
20^o INS +	$17^o.6$	1.87 ± 0.15	± 20^o	2.65	8.9	117100
Minimum Bias					5.9	54700

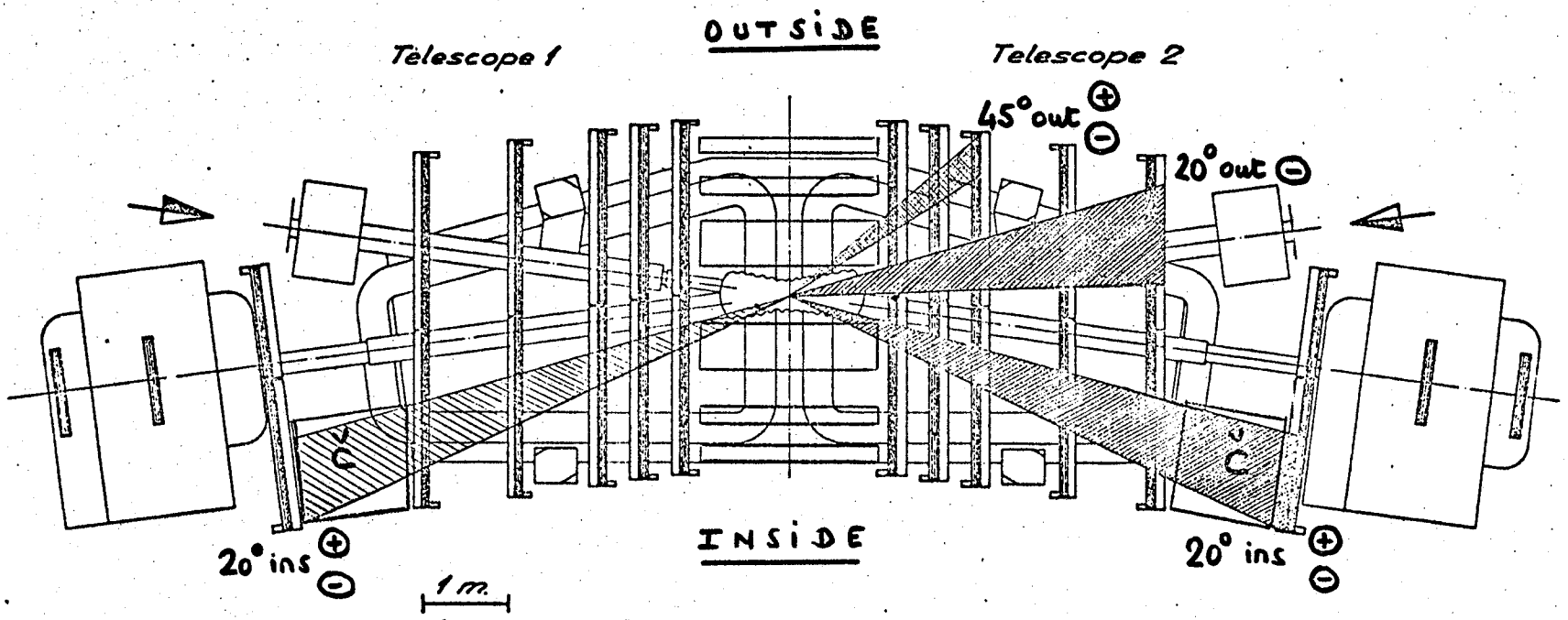
Telescope 1
OUTSIDE
Telescope 2
45° out ⊕ ⊖
20° out ⊖
C
C
20° ins ⊕ ⊖
1 m.
INSIDE
20° ins ⊕ ⊖

SFM

Fig.1

TOWARDS

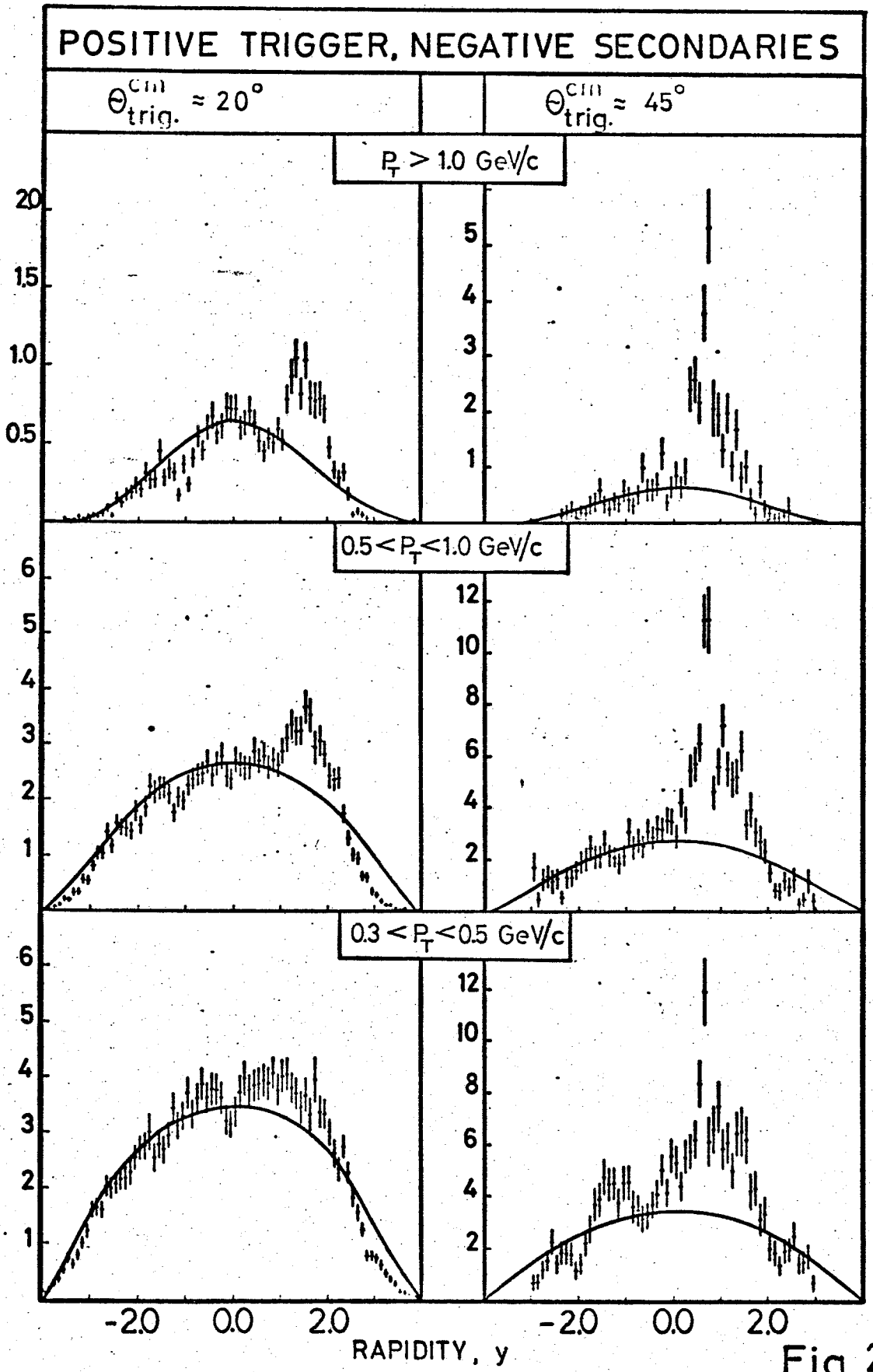

Fig. 2

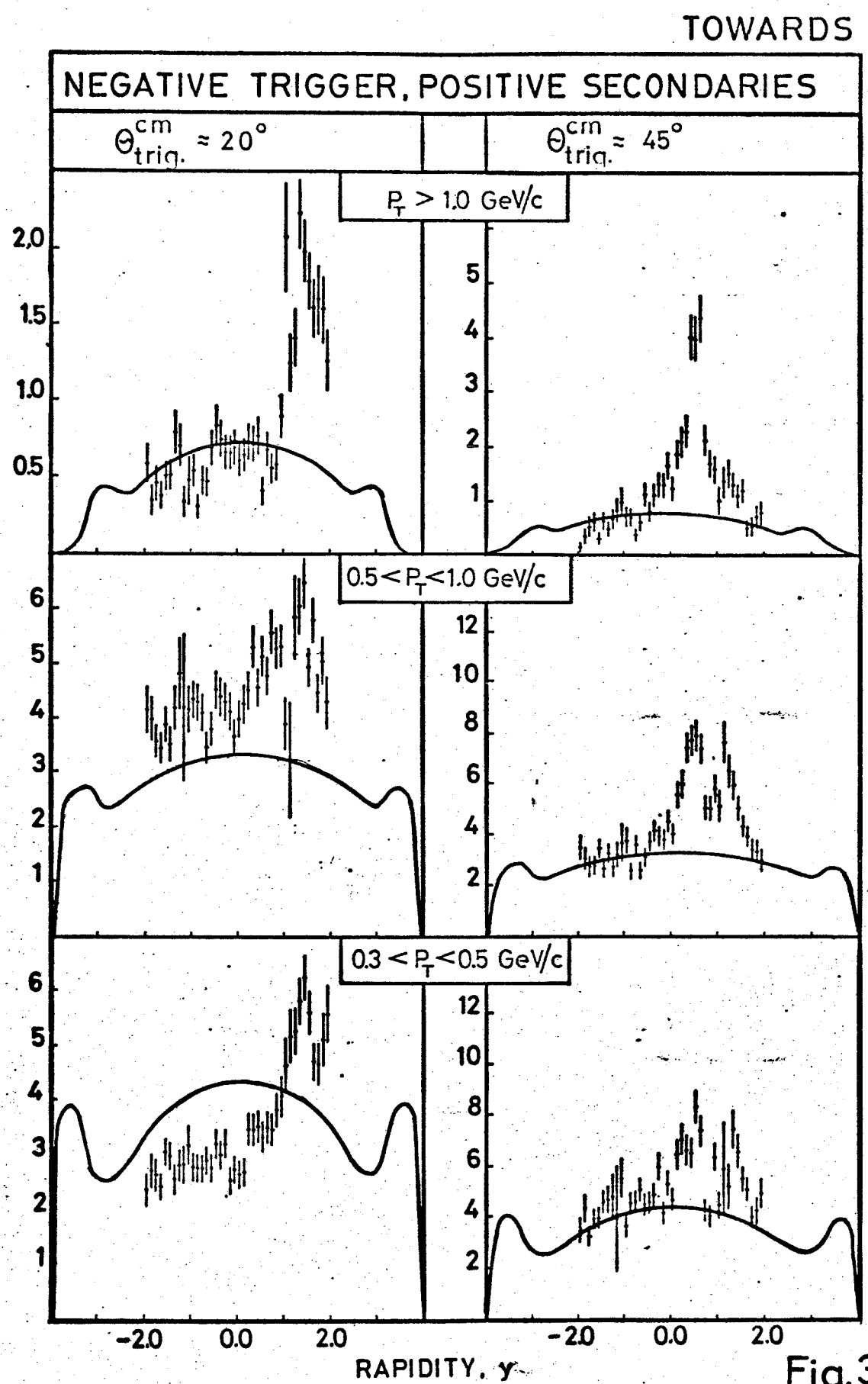
TOWARDS
NEGATIVE TRIGGER, POSITIVE SECONDARIES
$\Theta^{cm}_{trig.} \approx 20°$
$\Theta^{cm}_{trig.} \approx 45°$
$P_T > 1.0$ GeV/c
$0.5 < P_T < 1.0$ GeV/c
$0.3 < P_T < 0.5$ GeV/c
RAPIDITY, y
-2.0
0.0
2.0

Fig.3

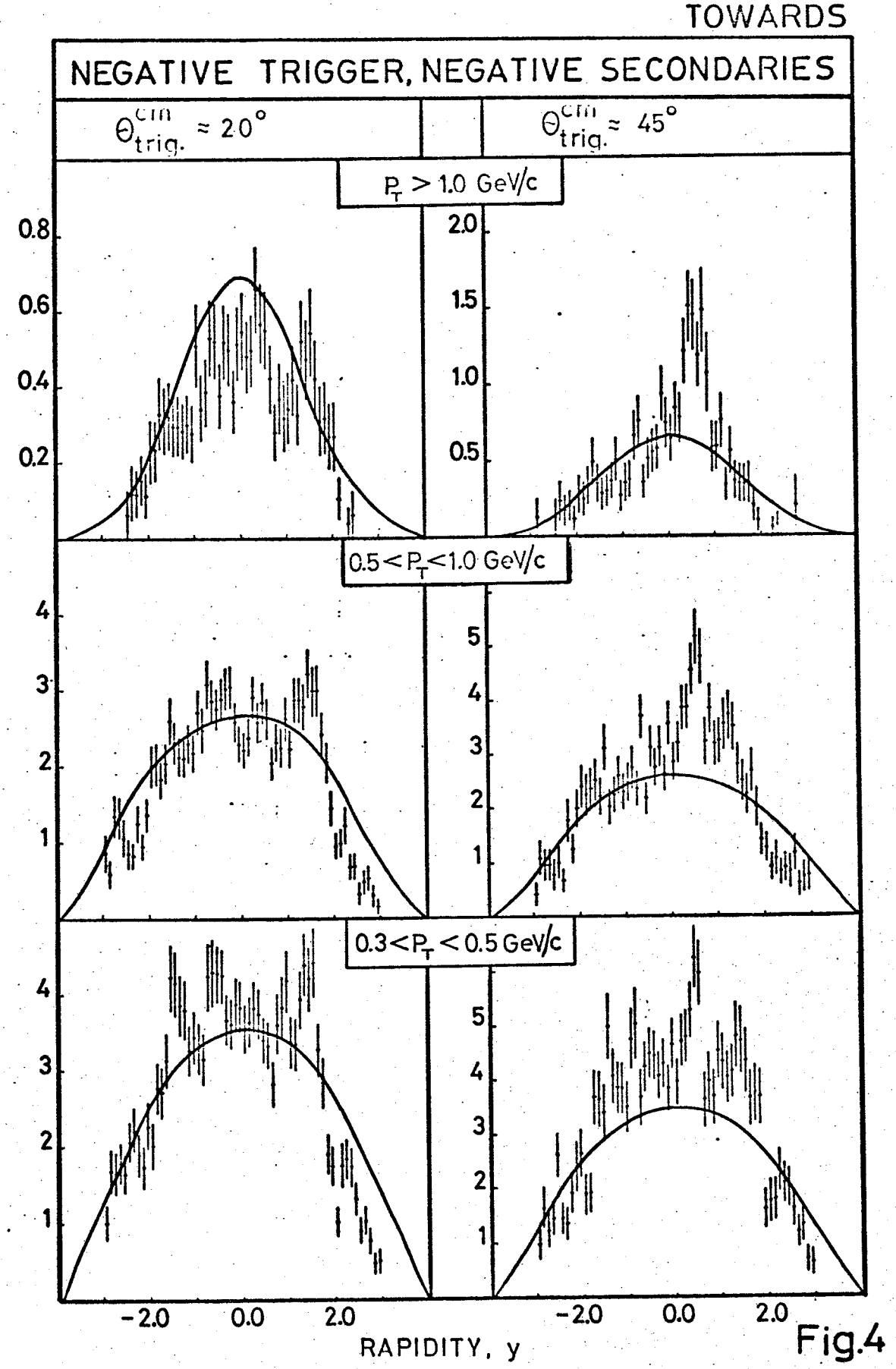
TOWARDS
NEGATIVE TRIGGER, NEGATIVE SECONDARIES
$\theta^{cm}_{trig.} \approx 20°$
$\theta^{cm}_{trig.} \approx 45°$
$P_T > 1.0$ GeV/c
$0.5 < P_T < 1.0$ GeV/c
$0.3 < P_T < 0.5$ GeV/c
0.8
0.6
0.4
0.2
2.0
1.5
1.0
0.5
4
3
2
1
5
4
3
2
1
-2.0
0.0
2.0
RAPIDITY, y

Fig.4

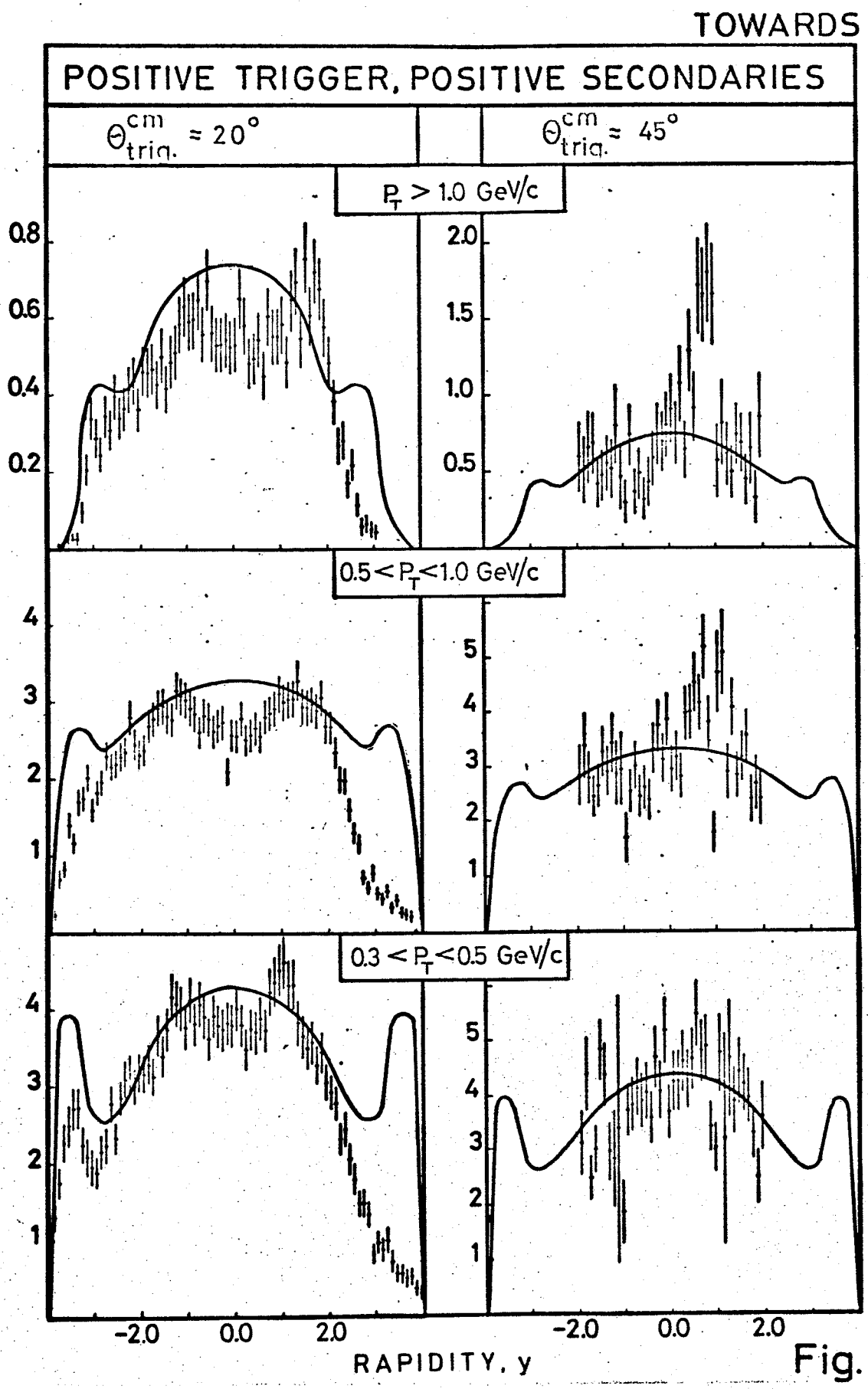
TOWARDS
POSITIVE TRIGGER, POSITIVE SECONDARIES
$\Theta^{cm}_{trig.} \approx 20°$
$\Theta^{cm}_{trig.} \approx 45°$
$P_T > 1.0$ GeV/c
$0.5 < P_T < 1.0$ GeV/c
$0.3 < P_T < 0.5$ GeV/c
0.8
0.6
0.4
0.2
2.0
1.5
1.0
0.5
4
3
2
1
5
4
3
2
1
-2.0
0.0
2.0
RAPIDITY, y

Fig.5

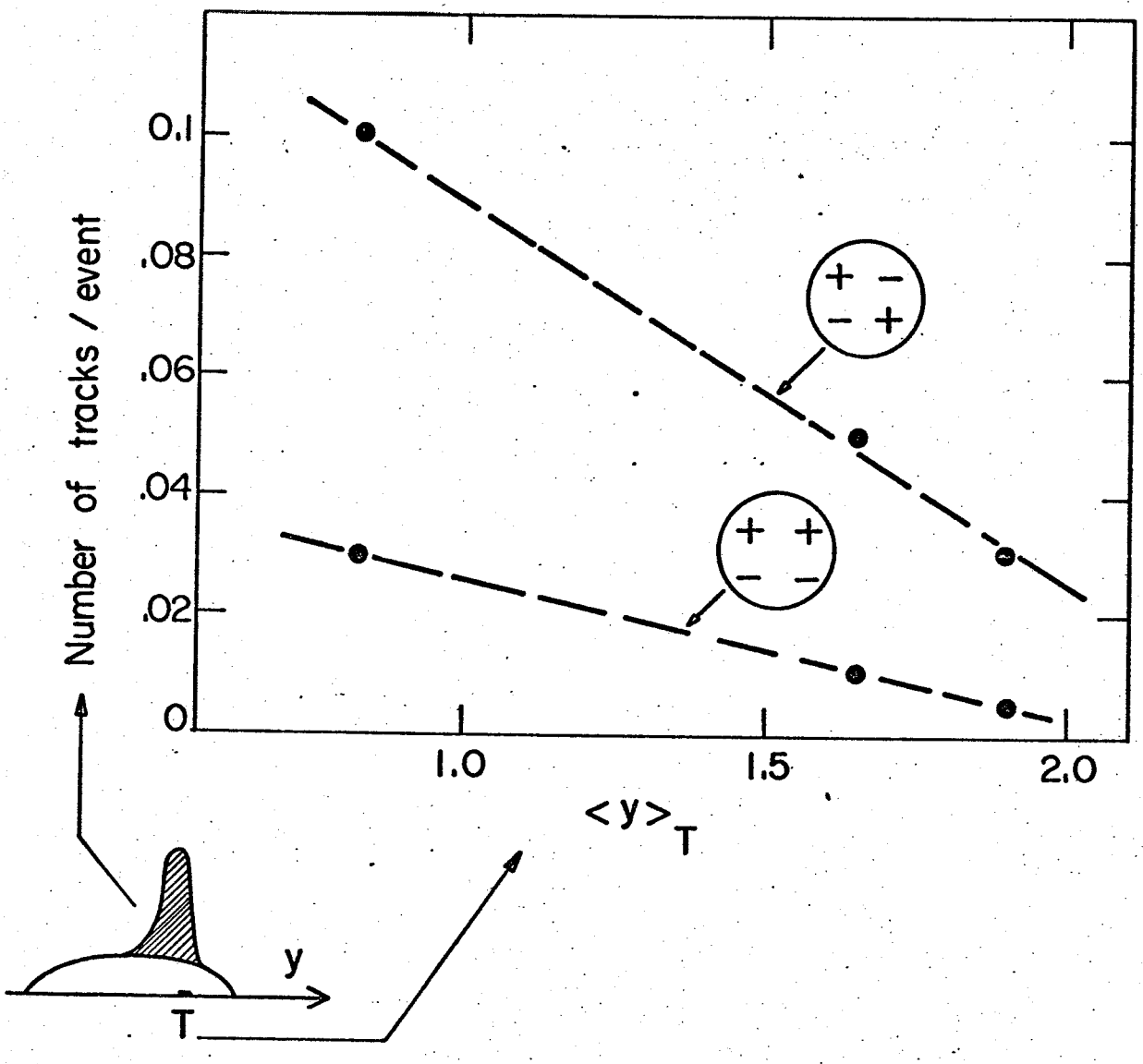

Fig.6

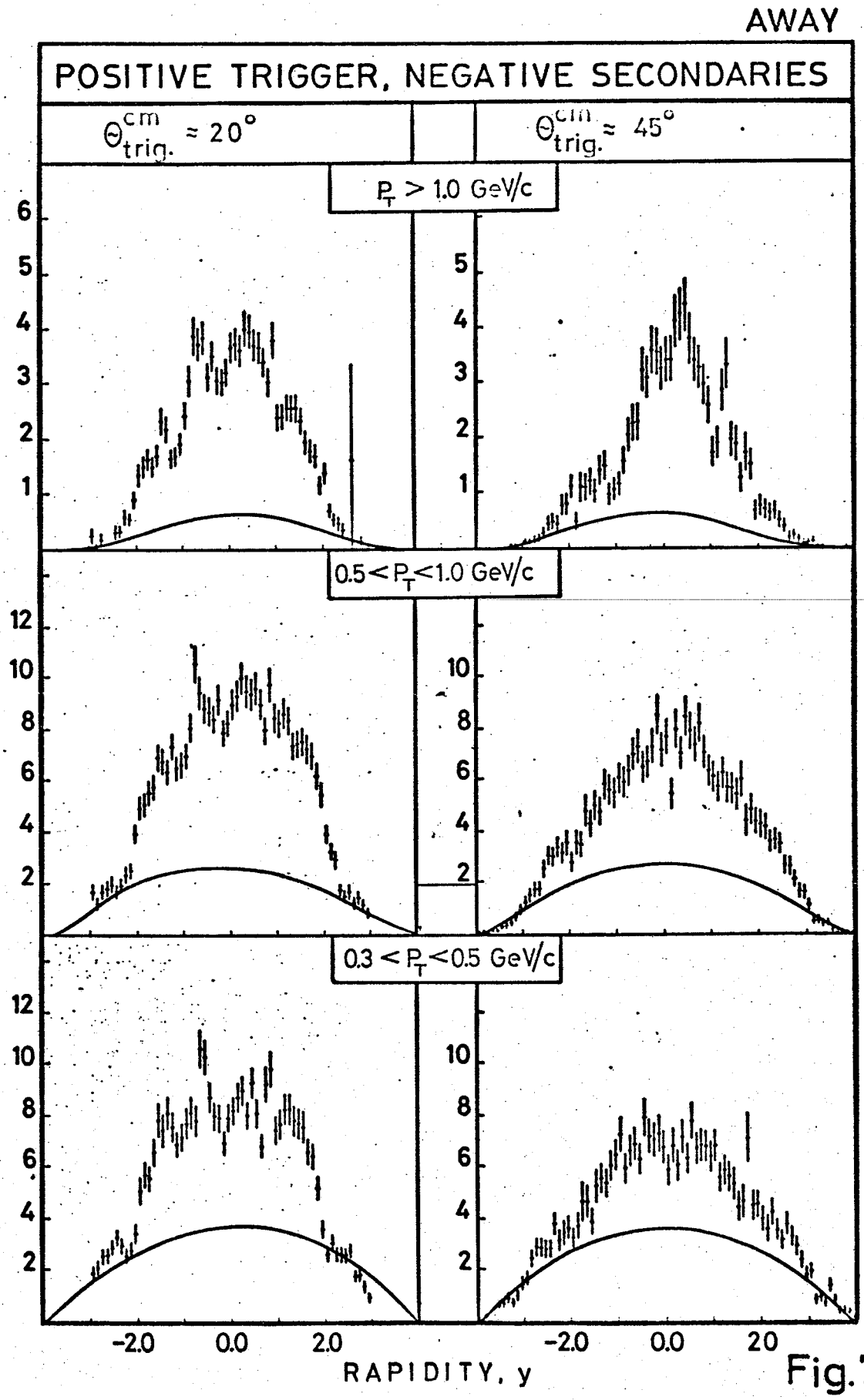
AWAY
POSITIVE TRIGGER, NEGATIVE SECONDARIES
$\Theta^{cm}_{trig.} \approx 20°$
$\Theta^{cm}_{trig.} \approx 45°$
$P_T > 1.0$ GeV/c
$0.5 < P_T < 1.0$ GeV/c
$0.3 < P_T < 0.5$ GeV/c
RAPIDITY, y

Fig.7

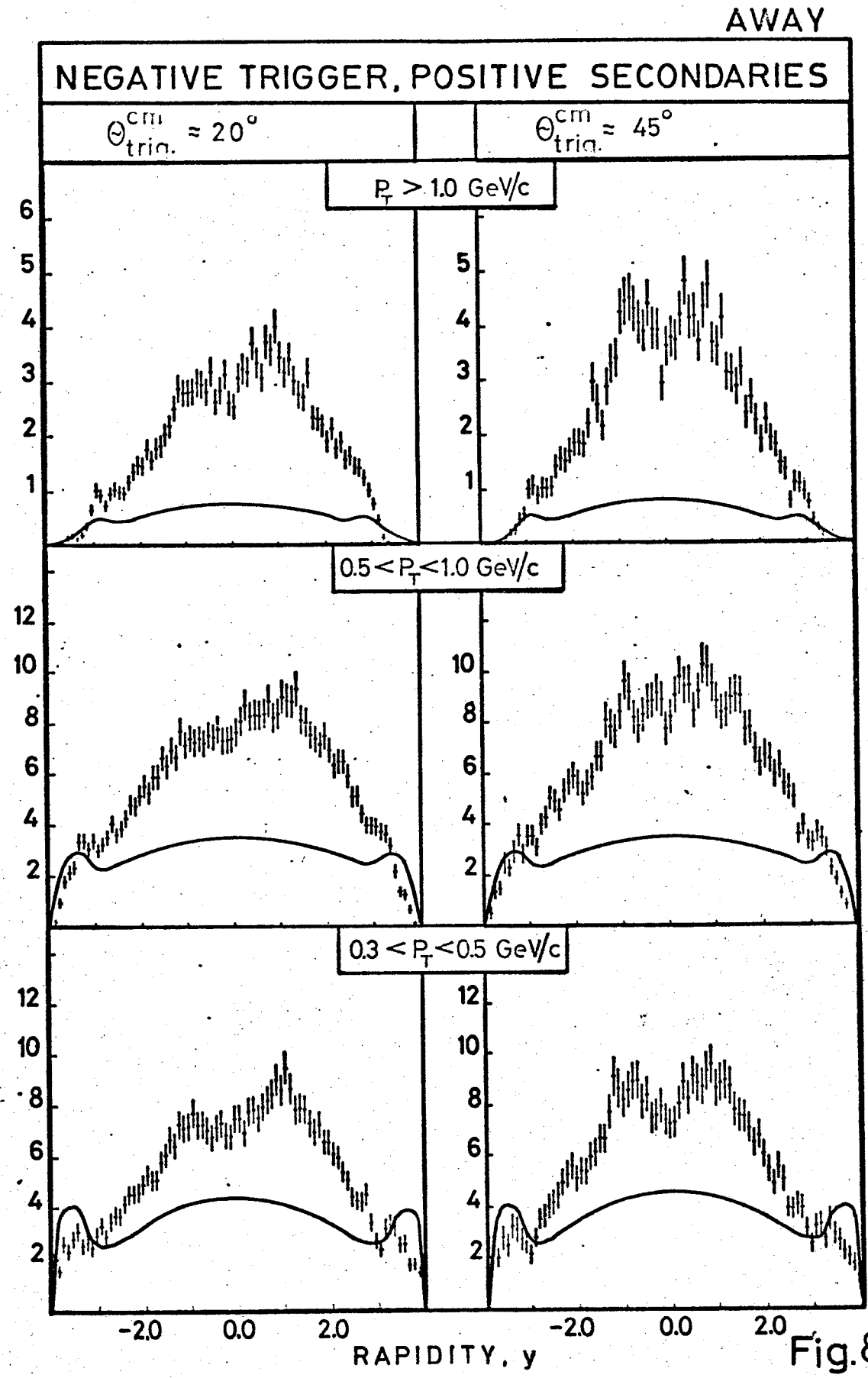
AWAY
NEGATIVE TRIGGER, POSITIVE SECONDARIES
$\Theta^{cm}_{trig.} \approx 20°$
$\Theta^{cm}_{trig.} \approx 45°$
$P_T > 1.0$ GeV/c
$0.5 < P_T < 1.0$ GeV/c
$0.3 < P_T < 0.5$ GeV/c
-2.0
0.0
2.0
RAPIDITY, y

Fig.8

AWAY

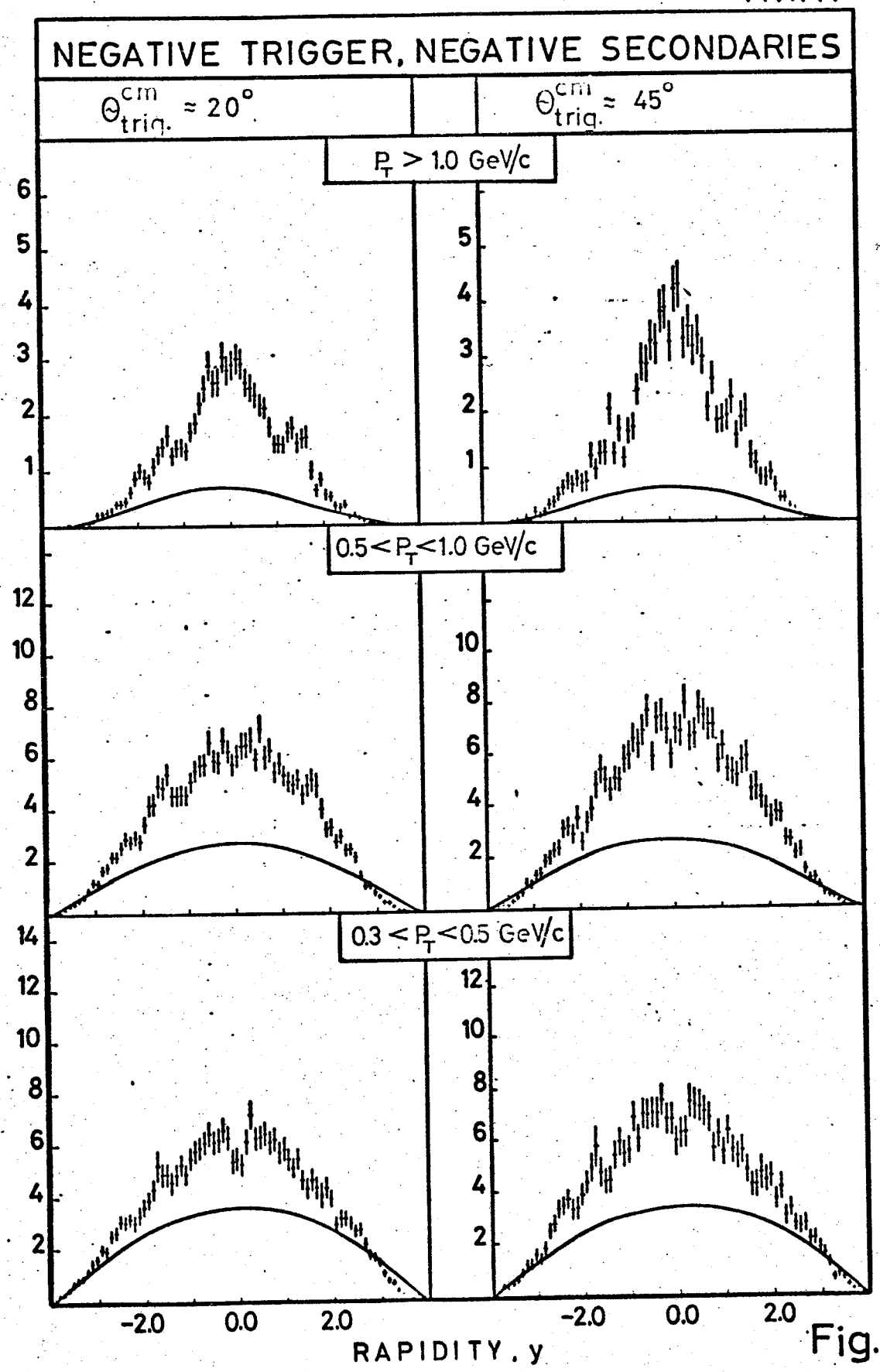
NEGATIVE TRIGGER, NEGATIVE SECONDARIES
$\Theta^{cm}_{trig.} \approx 20°$
$\Theta^{cm}_{trig.} \approx 45°$
$P_T > 1.0$ GeV/c
$0.5 < P_T < 1.0$ GeV/c
$0.3 < P_T < 0.5$ GeV/c
-2.0
0.0
2.0
RAPIDITY, y

Fig.9

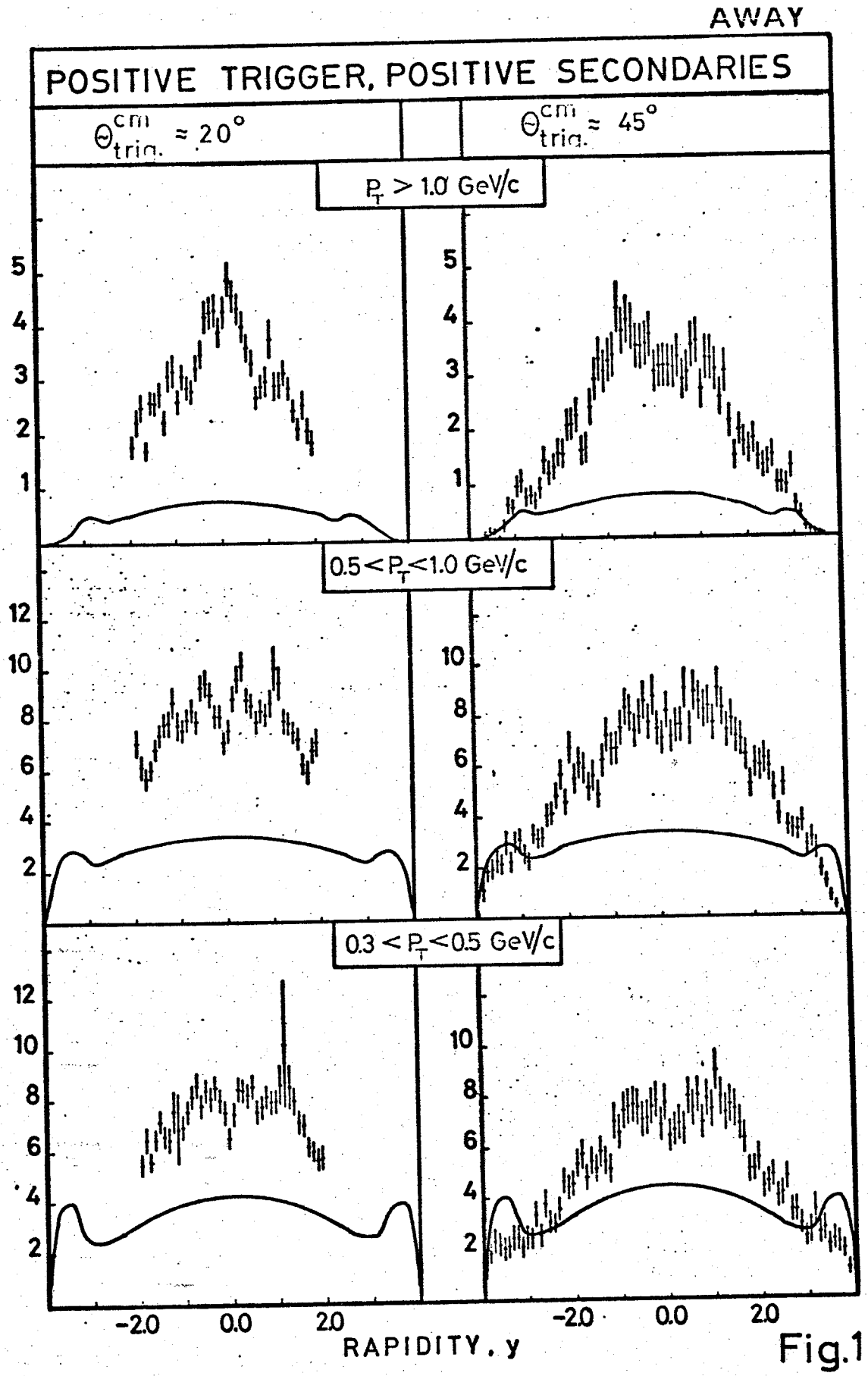
AWAY
POSITIVE TRIGGER, POSITIVE SECONDARIES
$\Theta^{cm}_{trig.} \approx 20°$
$\Theta^{cm}_{trig.} \approx 45°$
$P_T > 1.0$ GeV/c
$0.5 < P_T < 1.0$ GeV/c
$0.3 < P_T < 0.5$ GeV/c
-2.0
0.0
2.0
RAPIDITY, y

Fig.10